



## Retrofitting and Rehabilitation in Steel Moment-resisting Frame with Prestressed Concrete Slab against Progressive Collapse Potential

A. Shokoohfar\*, P. Kaafi Siyahestalkhi

Department of Civil Engineering, Qazvin Branch, Islamic Azad University, Qazvin, Iran

### PAPER INFO

#### Paper history:

Received 16 August 2021

Received in revised form 05 October 2021

Accepted 11 October 2021

#### Keywords:

Progressive Collapse Two-way Concrete Slabs

Finite Element Model Prestressed Slabs

Floor Openings

### ABSTRACT

Diaphragms are a fundamental part of the earthquake-resistant system, and in terms of rigidity, it is essential to transmit dynamic loads on a base of the structure. Also, floor openings on the response of buildings against progressive collapse are issues that have received less attention. In this study, floor opening surfaces and their positions on the progressive collapse potential of steel moment-resisting frame (SMRF) buildings were investigated according to the alternate load path method. Moreover, to retrofit and rehabilitate the two-way reinforced concrete (RC) slabs against a progressive collapse, two strategies, prestressed concrete slabs and installing carbon fiber reinforced polymer sheets on the surface of the old concrete slab, were proposed and six-story SMRF buildings were simulated using the finite element method. The maximum axial force around the removal column is 20% greater than the corresponding values on the floor opening is in the corner of the plan and the appropriate performance of the prestressed concrete slab leads to the load distribution in the ceiling diaphragm.

doi: 10.5829/ije.2022.35.01a.06

## 1. INTRODUCTION

Progressive collapse is a phenomenon in which one or several main members of a structure suddenly fail, and a total or a large part of it undergoes failure [1-3]. The mentioned initial damage in the above definition can occur in different members such as beams, columns, floors, load-bearing walls, etc. Although, the probability of these accidents occurring in ordinary buildings is not significant, this phenomenon becomes a critical and important issue when it may be with many humans, economic, and security losses.

Airplane impact, design or construction errors, fire, gas explosions, accidental overload, hazardous materials, vehicle collisions, bomb blasts, etc., are some of the unusual loads that can lead to the progressive collapse of buildings [4-6]. Because the probability occurrence of these hazards is low; they are not considered in the structural design or indirectly investigated by the passive defense protection measures. Most of these loads happen in a short period and lead to dynamic responses [7, 8].

Many buildings have suffered a progressive collapse in recent decades. Figure 1 demonstrates a timeline of the most important progressive collapse events all over the world. Mark's Campanile collapse [9], the University of Aberdeen Zoology building demolition in Scotland [10], the partial destruction of the Ronan Point tower in England [11], the destruction of the U.S. Embassy in Beirut in Lebanon [12], L'Ambiance Plaza progressive collapsed in the United States [13], Murrah building explosion in the USA [14], demolition of Sampoong department store in South Korea [15], progressive collapse of Khobar Towers in Saudi Arabia [16], airstrikes on world trade center tower in the USA [17], demolition part of the Tropicana Parking Garage in the USA [18], demolition part of Saadatabad building in Iran [19], demolition of Margalla towers in Pakistan [20], demolition of Plasco building in Iran [6] and demolition part of Beirut buildings in Lebanon [21] are the progressive collapse events that can be mention. The above-mentioned events have resulted in deaths and injuries of significant number of human beings. A review

\*Corresponding Author Email: [ahmadshokoohfar@gmail.com](mailto:ahmadshokoohfar@gmail.com) (A. Shokoohfar)

of other similar accidents worldwide showed that the progressive collapse potential of buildings could be decrease by safety improvement, repairing, and strengthening damaged structures. The timeline of the most important progressive collapse events all over the world is shown in Figure 1.

Numerous studies have been performed on progressive collapse. Each study evaluated part of this phenomenon. Many studies have been performed to investigate the contribution of structural members such as beams and columns in the vicinity of the removed column and the effect of different lateral bearing systems against progressive collapse [22-30]. In other studies, different types of progressive collapse analysis methods were investigated [31-38]. Several researchers investigated different types of beam-column connections on the response of concrete and steel structures against progressive collapse [39-43]. On the other hand, various studies were conducted to evaluate the vulnerability of masonry buildings, and the importance of rehabilitation of these structures was raised [44-46].

Ozturk et al. [47] studied the retrofit methodology by adopted fiber reinforced polymers (FRP) material on the existing building, analysis results showed that there are improvements in stable maximum drift due to apply of FRP as compared with the control building. Ozturk. [48, 49] studied the focuses on a displacement-based approach for analyzing the seismic behavior of two monumental buildings located in the historical

Cappadocia region of Turkey. Modal, response spectrum, and dynamic analyses for different ground motions were applied to these building models. It is observed that slab discontinuities on the gallery floor constitute a major element in the structural damage expected for the building.

Various studies were performed on the response of steel moment-resisting frames (SMRFs) against progressive collapse. The response of SMRFs against various scenarios of progressive collapse due to fire was investigated. Dynamic analysis was used for this purpose. A method was proposed to consider the heat caused by a fire in the progressive collapse process [50]. The progressive collapse behavior of steel frames with different beam-column connections was investigated. The results showed that welded flange plate (WFP) connections have higher flexural strength than bolted [51]. Beam-column connections with reduced cross-section against progressive collapse were investigated. The results showed that in connections with reduced cross-sections, the diameter and distance of the web openings are among the important parameters that affect structure response against progressive collapse [52]. Progressive collapse due to a fire in the Plasco building in Tehran (Iran) was investigated. The results showed that the building vulnerability was due to insufficient ductility and structural continuity, which led to the spread of damage to the entire structure [6]. The vulnerability of

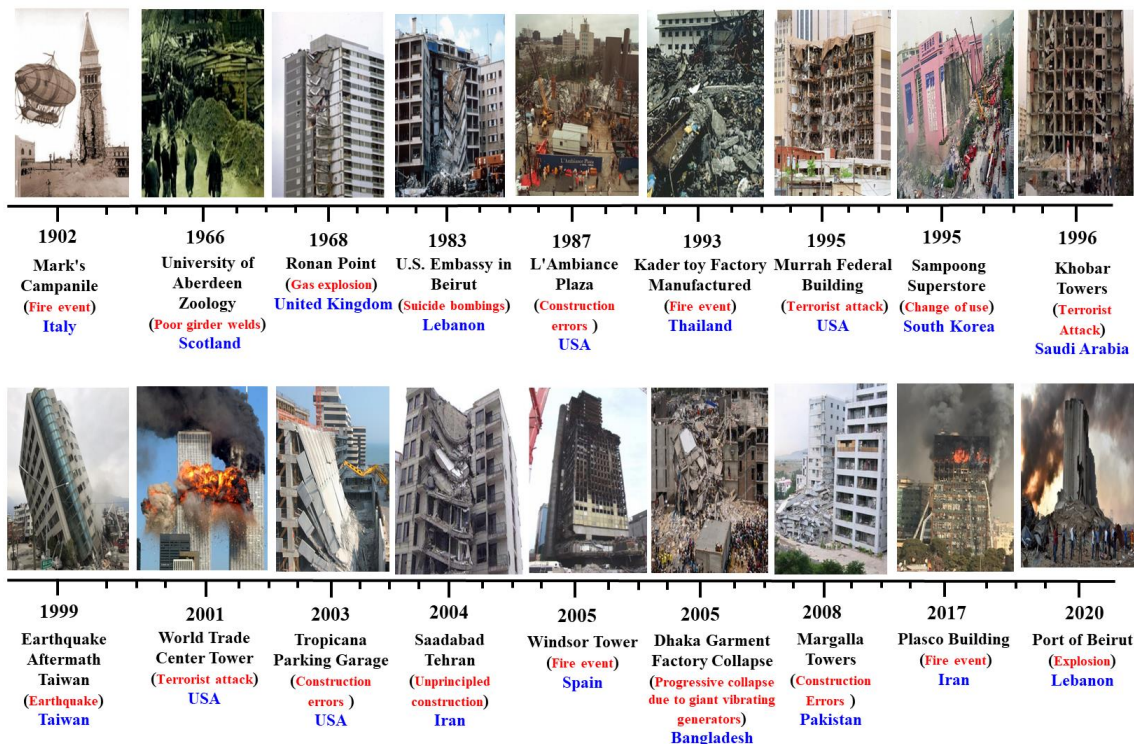


Figure 1. Timeline of the most important progressive collapse events all over the world

buildings with irregular voided located in seismic areas was investigated. The results showed that the structures situated in high seismic zones could pass progressive collapse analyses. The seismicity level of the site is more important than another parameter, such as the height or irregularity of the structure [45].

One of the important members of the structure that has been less studied than other members is the effect of the floor contribution on the strength of the structure to progressive collapse. The floor system is one of the elements that resist progressive collapse due to removing the column.

The roof system of many old steel buildings must be retrofit. The seismic performance of the old steel structures depends on the quality of the welding procedure and the tensile strength of the steel used. With proper welding quality and proper material specifications, there are several major disadvantages in older steel buildings that cause severe earthquake damages. The brick arch panels are generally used as floor systems in the old steel buildings of Iran. These floors were composed of steel beams and compression bricks. The brick arches are not well in earthquakes due to the lack of integration and high weight. An example of these buildings is shown in Figure 2. Flexural forces redistribution and the shear response, interaction with columns for increasing frame performance, and membrane performance are factors that can affect the redistribution of gravitational forces in the damaged buildings. Immediately after the column's destruction, the column bends, bending cracks, rebar yielding of the slab occur, and the beam forces increase [54]. These axial compressive forces can have a major effect on the flexural behavior and changes in the vertical load-bearing capacity of the beams. The forces created inside the roof diaphragm help reduce the vertical displacement of the top point of the removed column and thus help to improve the behavior of the structure against progressive collapse.

In fact, today, openings are created in the building floors in many buildings due to architectural considerations. Since in the studies of progressive collapse, little attention has been paid to the effect of

opening on the floors with reinforced concrete (RC) slabs, in the present study, this issue is investigated. On the other hand, the slab opening leads to a change in the structural response of progressive collapse. Thus, in the present study, by simulating the opening in RC slabs and changing the dimensions and position of these openings in SMRF buildings, the effect of size and opening position on the resistance of the SMRF buildings against progressive collapse will be investigated.

Most modeling to progressive collapse using software analysis was investigated. Engineers' familiarity with this software doubles the need to clarify vague angles of modeling this phenomenon in such software. ABAQUS [55] software has a more prominent position among this software due to its suitable capabilities. However, little research has been done on floor modeling in this software in the face of progressive collapse. In most modeling, the effects of the floor simulation on progressive collapse have been ignored. In this study, the effect of definable characteristics of floor diaphragm in ABAQUS software was applied for progressive collapse analysis of SMRF buildings. Two strategies of retrofitting and improvement of floor diaphragm were proposed.

Prestressed concrete slabs were used for rehabilitation, and their performance was compared with conventional reinforced concrete (RC) slabs. Prestressing is a method of reinforcing concrete or other materials with high-strength steel strands or rebars. Concrete slabs based on prestressing methods have significant architectural, structural, and economic advantages. Thus, one of the most important objectives of the present study is to investigate the effect of slab prestressing on the progressive collapse of steel buildings. Carbon Fiber Reinforced Polymers (CFRP) can increase the load-bearing capacity of the structure, improve the building performance in bearing live loads or restore the lost strength of the floor and slab due to steel corrosion. The results of previous studies have shown that the strength of the floor and slab significantly improves after retrofitting with CFRP, and they can be easily glued over concrete floors and slabs due to low thickness and easy installation. Retrofitting of floor and slab with CFRP can also act as insulation and increase the structure's load-



**Figure 2.** Demolition of the brick arch panel in a steel building to strengthen in Iran

bearing capacity and achieve the desired performance in the structure. Strengthening the floor and slab with CFRP increases the shear and flexural strength, and It retrofits the structure against corrosion, vibration, and abrasion and ultimately improves the performance level of the structure against earthquakes [56-62]. Due to the mentioned advantages in the present study and several cases, CFRP sheets are used to increase the resistance of the floor slab against progressive collapse. The flowchart of the study process is shown in Figure 3. Details and variables are presented in the next section.

## 2. INTRODUCING THE STUDIED BUILDINGS

Variables include floor opening position (corner and middle of plan), floor opening dimensions (4000×10000 and 6000×12000 mm), and floor slab condition (two-way RC slab, prestressed reinforced concrete slab, retrofitting two-way RC slab with CFRP). For this purpose, six-story SMRF buildings were modeled and analyzed in Figure 3.

All modes are summarized in Table 1. All the buildings have the same plan, and the height of each story was considered 3200 mm. The building lateral load-bearing system is an intermediate moment-resisting frame in both x and y directions. The plan dimensions of the studied buildings and the location of the openings are shown in Figure 4. The steel used is St37 building steel with 370 MPa ultimate strength and 240 MPa yielding strength. Etabs [63] software and load-resistance factor design were used for modeling and analysis. The importance level of buildings concerning residential use is medium importance. Two-way RC slabs were considered as floors in the initial design. The thickness of

the concrete slab was 250 mm, and reinforcing bars with a diameter of 14 mm was used at intervals of 150 mm.

The dimensions and specifications of the designed sections are presented in Table 2. The beam cross-sections of the first to the third floor, fourth to the fifth floor, and sixth floor were considered IPE550, IPE500, and IPE450, respectively. Also, the cross-sections of the columns for the first to second levels Box400×400×30, for the third to fourth levels Box400× 400×20 and the fifth and sixth levels Box400×400×14 were considered. After determining the beams and columns sections, all the buildings were simulated in three dimensions using ABAQUS software. Etabs is an advanced software in building modeling. Still, due to some limitations, such as the inability to simulate concrete slab cracks and very low outputs, the phenomenon of progressive collapse cannot be simulated using this software. Nonlinear dynamic analysis by direct integration method was used to evaluate the progressive collapse. Details of finite element simulation are provided below. The results of studies on progressive collapse show that the corner columns removal on the ground floor leads to far more critical responses [64-66]. Thus, in all cases, A1 and B1 columns on the ground floor were removed.

## 3. FINITE ELEMENT SIMULATION

The structural elements considered in this research include beams, columns, two-way RC slab, prestressed slabs, and CFRP. The beam and column sections were defined using the Beam element, and steel rebar was used wire. Also, concrete slab and CFRP sheets were defined using shell elements. In this study, the concrete damage plasticity model (CDPM) was used to define concrete.

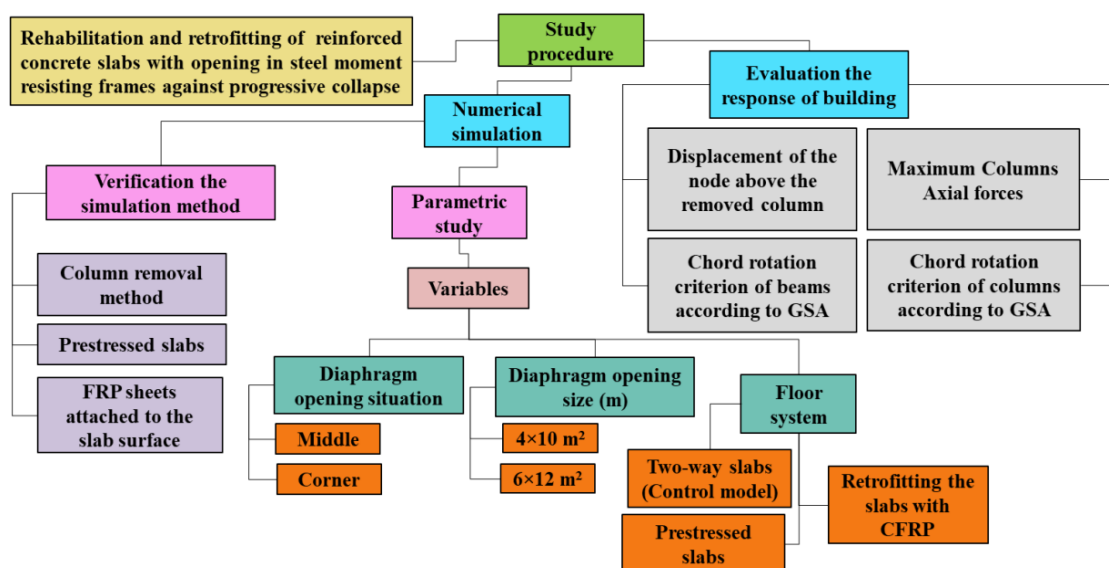


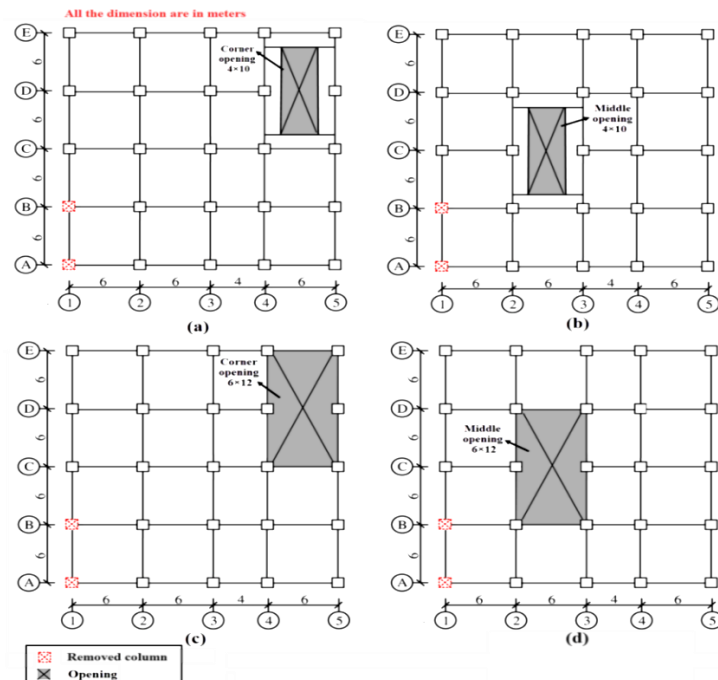
Figure 3. Research process

**TABLE 1.** Introducing the investigated cases

Case	Floor opening situation	Floor opening size (m)	Concrete slab type	Columns removed at ground floor
1	Corner	4×10	Two-way RC slabs	A1 & B1
2	Middle	4×10	Two-way RC slabs	A1 & B1
3	Corner	6×12	Two-way RC slabs	A1 & B1
4	Middle	6×12	Two-way RC slabs	A1 & B1
5	Corner	4×10	Prestressed RC slabs	A1 & B1
6	Middle	4×10	Prestressed RC slabs	A1 & B1
7	Corner	6×12	Prestressed RC slabs	A1 & B1
8	Middle	6×12	Prestressed RC slabs	A1 & B1
9	Corner	4×10	Retrofitting RC slabs with CFRP	A1 & B1
10	Middle	4×10	Retrofitting RC slabs with CFRP	A1 & B1
11	Corner	6×12	Retrofitting RC slabs with CFRP	A1 & B1
12	Middle	6×12	Retrofitting RC slabs with CFRP	A1 & B1

**TABLE 2.** Column and beam sections

Case	Designation	Flange thickness (mm)	Web thickness (mm)	Width (mm)	Depth (mm)	Mass/meter (kg/m)
Beam sections	IPE400	13.5	8.6	180	400	66.3
	IPE450	14.6	9.4	190	450	77.6
	IPE550	17.2	11.1	210	550	106
Column sections	Designation	Thickness (mm)	Width (mm)	Mass/meter (kg/m)		
	Box450×450×30	30	450	200.2		
	Box350×350×30	30	350	157.8		
	Box300×300×30	30	300	134.2		

**Figure 4.** Typical plan layout of the model with different floor opening situation (a) Corner opening (4×10 m) (b) Middle opening (4×10 m) (c) Corner opening (6×12 m) (d) Middle opening (6×12 m)

This section considered the characteristics of damage index in compression (dc) and tension (dt). The parameters are shown in Figure 5.

The CDPM is based on similar damaged and is designed for concrete under ideal loadings. The effect of reducing elastic hardness resulting from plastic strains under both tension and pressure is considered in this model. The development of stiffness recovery effects during loads is also considered. Due to the fact that in the concrete damaged plasticity model, the concrete properties are defined both under tension and pressure for the program, and this model can consider the effect of reducing concrete hardness affected by hysteresis loading. Therefore, the concrete damaged plasticity model is the most suitable option for beam modeling in this project. The detailed analysis of this model and its parameters are discussed in Equations (1-3).

$$\varepsilon_t^{cr} = \varepsilon_t - \varepsilon_t^{el} \tag{1}$$

$$\varepsilon_t^{el} = \frac{\sigma_t}{E_0} \tag{2}$$

$$\varepsilon_t^{~pl} = \varepsilon_t^{~ck} - \frac{d_t}{(1-d_t)} \frac{\sigma_t}{E_0} \tag{3}$$

To define the elastic behavior of rebar, it is necessary to define the elastic modulus and the Poisson's ratio, equal to 210000 MPa and 0.3, respectively. The density of steel was considered 7850 kg/m<sup>3</sup>. However, this behavioral phase is responsible for small applied loads. To determine the exact behavior of materials at large applied loads, it is necessary to define the yield and ultimate point. The used steel is St37 building steel. For steel components, the strength such as the yield point is 240 MPa, and the strength such as the failure point is 370 MPa. The characteristics of the materials used in the present study are given in Table 3. The model's damping coefficient was 5%—used Riley's method to define the

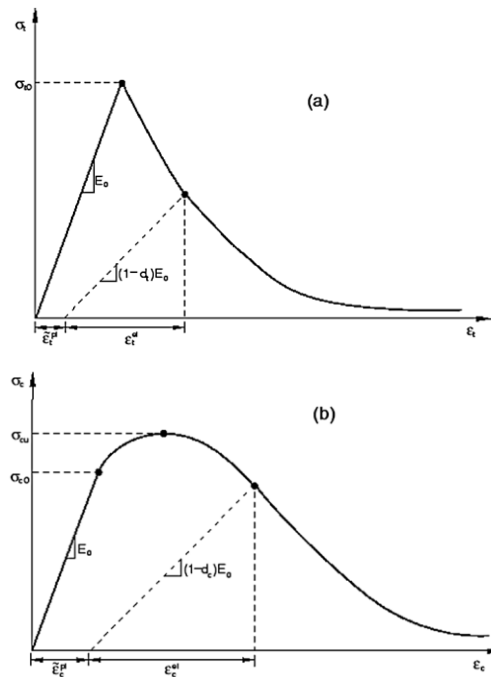


Figure 5. CDPM parameter, (a) tension (b) compression

damping of the structure. By extracting the alternation times of the structure and calculating its natural frequency, the mass damping coefficient ( $\alpha$ ) and the stiffness damping coefficient ( $\beta$ ) according to Equation (4) were obtained and defined in ABAQUS software.

$$\zeta = \frac{\alpha}{2\psi_n} + \frac{\beta\psi_n}{2} \tag{4}$$

Shell and Truss's elements were used for S4R and T3D2 meshing, respectively. To determine the optimal mesh in modeling used the method of examining the convergence of the responses. According to Figure 6, the structure was analyzed, and to correct the mesh method, collected the maximum stress in beam and column in structure. The mesh in the present study is considered to be 80 mm.

TABLE 3. The mechanical properties of materials (Units: Newton, Meter)

Concrete	Young's modulus	Poisson's ratio	Plasticity parameters of concrete				Viscosity parameter
			Dilation angle ( $\psi$ )	Eccentricity (m)	$F_{bo}/f_c$	Kc	
	$3 \times 10^{10}$	0.2	31	0.1	1.16	0.667	0.001
	Young's modulus	Poisson's ratio	Yield strength	Tension strength	Elongation (%)	Equivalent diameter	
Steel	$2.1 \times 10^{13}$	0.3	$390 \times 10^6$	$560 \times 10^6$	30	---	
Prestressed Steel	$1.8 \times 10^8$	0.3	$16.87 \times 10^8$	$18.11 \times 10^8$	3.5	$13.35 \times 10^{-3}$	
	Young's modulus	Poisson's ratio	Thickness	Tension strength	Elongation (%)		
CFRP	$10075 \times 10^7$	0.22	$11 \times 10^{-5}$	$4200 \times 10^6$	1.8		

The distribution of the loads by the prestressed cables in each direction depends on the support distance in different directions. The prestressing force of cables was obtained according to Equation (5):

$$P = q \cdot r \tag{5}$$

In this relation,  $q$  is the amount of external load perpendicular to the cable in width of one meter, and  $r$  is the average radius of curvature of the cable. In the case of using cables with the relatively low friction coefficient and length of 30 to 40 meters, the area of prestressed cable with a suitable approximation of Equation (6) is obtained:

$$A_p = \frac{p}{0.95 \times 0.65 \times f_{pk}} \tag{6}$$

$f_{pk}$  is the amount of stress on the prestressed cable.

According to the used cables, the limit stresses due to friction are obtained from Equation (7):

$$P_x = P_j \times e^{-(\mu\alpha + Kx)} \tag{7}$$

where,  $P_x$  = Stress at distance  $x$  from the jacking point,  $P_j$  = stress at jacking point,  $\mu$  = coefficient of angular friction,  $\alpha$  = total angle change of the strand in radians from the stressing point to distance  $x$  (Figure 7),  $K$  = Wobble coefficient of friction expressed (rad. per meter).

The initial step is to simulate prestressed axial load and the initial tensile stress applied to the rebars. To transfer the prestressing of the rebar to the concrete slab, the stresses were applied in the initial step, and in the next steps, the applied tensile stresses cause pressure in the concrete slab (Figure 8).

Dynamic Explicit analysis was used for nonlinear dynamic analysis, and this type of analysis makes it possible to define general contact conditions and apply large deformation theory. For this purpose, two steps are defined: the first step of prestressed loading and the second step by gravity loading in structure. Tie constraints were used to define interaction and contact between all surfaces [7, 8]. This constraint allows combining two surfaces whose meshes are different from each other and is one of the most widely used constraints in civil engineering.

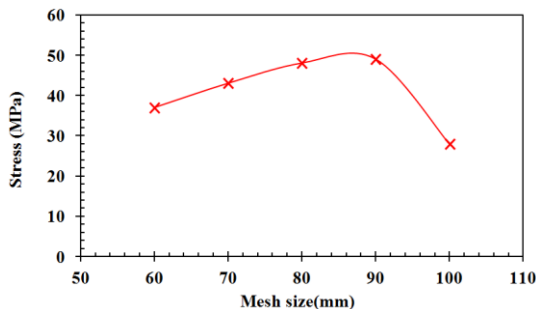


Figure 6. Mesh sensitivity analysis of the studied steel structures

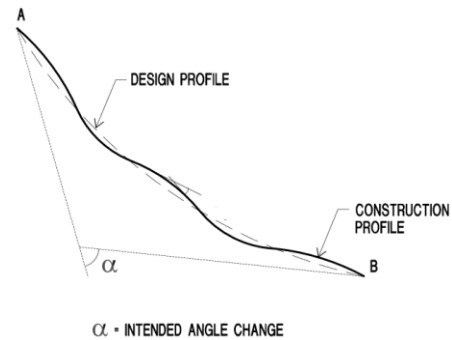


Figure 7.  $\alpha$  parameter in prestressed cable relations

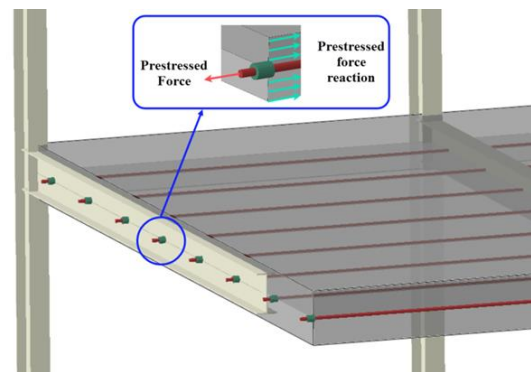


Figure 8. Simulation of prestressed slab floor in SMRF buildings

For gravitational loading of the structure, in addition to the gravitational force of the ground, a load combination related to progressive collapse was applied. In nonlinear dynamic analysis, the removal column is not modeled from scratch. Unlike nonlinear static analysis, in nonlinear dynamic analysis, the internal loads of the column removal site must be applied to the top of the removed column to be applied in one step under another impact load and zero the column load. To define the supports, the end of the columns was tied in all directions, and movement and rotation were prevented. To simulate the sudden removal of the column, columns B1 and A1 were first removed from the model. The internal forces of the column were applied in the opposite direction at the location of the column node. According to UFC2009, the removal time of these forces must be less than 0.1 vertical rotation time of the structure in the vertical movement mode above the column. In this study, to define the boundary conditions, the ends of all columns are defined as fixed. This support prevents movement and rotation. The loads applied to the structure include the weight of the structural components (beams, columns, and slabs), dead and live loads on the structure floor, and the progressive collapse potential was Evaluate by considering the alternative load path model. In this method, the structure is designed so that if a member is removed and the load transfer path is damaged, there are

other alternative paths for transferring the load to the ground. Thus, structures are designed to remove special columns or walls [2]. The assessment of progressive collapse potential was performed using the alternative load path method, independent of the collapse factor, and proposed by GSA and DOD [1]. The removal site columns in the studied models were removed for modeling in the software, and loading was done according to UFC regulations [1]. The applied loads were applied to the studied models as a combination of the following loads.

- Gravity load increased was used for the floors above the removed columns. This combination of load should be affected in the form of intensified gravity load as follows on the openings adjacent to the removed elements in all floors above these elements:

$$G_{LD} = \Omega_{LD}[(0.9 \text{ or } 1.2) D + (0.5L \text{ or } 0.2S)] \quad (8)$$

$G_{LD}$  = Gravitational intensified load for deformation-controlled efforts in the linear static method

D = Dead load considering the exponential load

L = Live load

S = Snow load

$\Omega_{LD}$  = increase coefficient to calculate the deformation control effort

- And the gravitational load on the other surfaces of the roof is obtained from the following equation with the G load combination:

$$G = [(0.9 \text{ or } 1.2) D + (0.5L \text{ or } 0.2S)] \quad (9)$$

In this Equation (9), G is gravity load.

#### 4. VALIDATION

Validation is done to ensure the output results of ABAQUS software. Because in this software, there are many options for modeling geometry, the interaction between components, loading method, etc., and changing each of them can vary the analysis results. Thus, by comparing the results of the experimental samples with the ABAQUS numerical models; it can be shown that the modeling is correct. Then, new results can be obtained by changing the parameters. Three parallel issues were investigated in the present study: progressive collapse due to removing the column in steel buildings, simulation of prestressed concrete slabs, and simulation of CFRP sheets installed on concrete surfaces. Thus, three different laboratory studies were selected and simulated using the used simulation method in the present study.

##### 4. 1. Investigation Accuracy of the used Method for Column Removal (Alternative Load Path Method)

The accuracy of the simulation method used in column removal was evaluated by simulation of an experimental frame made in the study of Guo et al. [67]. The frame has one floor and four spans made in the laboratory with a

1:3 scale. The length and height of each frame span were considered 2 and 1.20 meters, respectively. The steel beams were completely welded to the flange of the columns as the beam-column connections have rigid. The cross-section of the beams was H 200×100×5.5×8, and the cross-section of the columns was H 200×200×8×12. (Numbers after H in order are: d: total height of section; bf: flange width; tw: web thickness; tf: flange thickness). The slab's width and depth were 800 and 100 mm, respectively. The steel percentage of reinforcement mesh was considered 0.85%. Longitudinal reinforcement bars with a diameter of 12 mm were placed in two layers at equal distances along the slab width. Also, transverse reinforcing bars were used with 8 mm diameter in the steel reinforcement mesh to prevent concrete failure. To simulate the column removal, the middle column also has no support. The column's bottom was welded to a beam attached to the ground to create fixed support. The behavior of the frame and the concrete slab was evaluated during the test. For this purpose, a linear variable differential transformer (displacement sensor or LVDT) was placed vertically in the middle of the frame at the column C location. Also, four displacement sensors were used to measure the displacement of columns A, B, D, and E. A hydraulic jack with 500 kN load capacity was used on the top of column C for applying vertical load. Also, a 1000 kN load measuring device was used to measure the vertical load. Using this method and the mentioned devices, it was easily possible to investigate the redistribution and transmission of internal force after removing the frame middle column. The load was applied according to JGJ 101-96 [68].

The load-deflection controlling method was used until the frame reached ultimate capacity. The load-deflection diagram of the laboratory sample, the models of Guo et al. [67] and the present study is shown in Figure 9. The maximum load and corresponding deflection in the laboratory study were 400 kN and 440 mm, respectively. The maximum load in the finite element study with ABAQUS software was also done by Guo et al. [67]. It is 450 kN, with a corresponding displacement of approximately 500 mm. The maximum load of the model simulated by the method used in the present study is 412 kN, with a corresponding deformation of approximately 452 mm. Thus, the maximum displacement values and ultimate load in the finite element modeling method used in this study, which was performed using ABAQUS software, have a relatively good accuracy compared to the laboratory study.

##### 4. 2. Evaluation of the used Method Accuracy in Simulating CFRP Sheets Installed on Reinforcement Concrete Slab

This section investigated the validation of the finite element method (FEM) used to simulate CFRP sheets installed on reinforcement concrete slab. For this purpose, a reinforced concrete slab made in the laboratory study

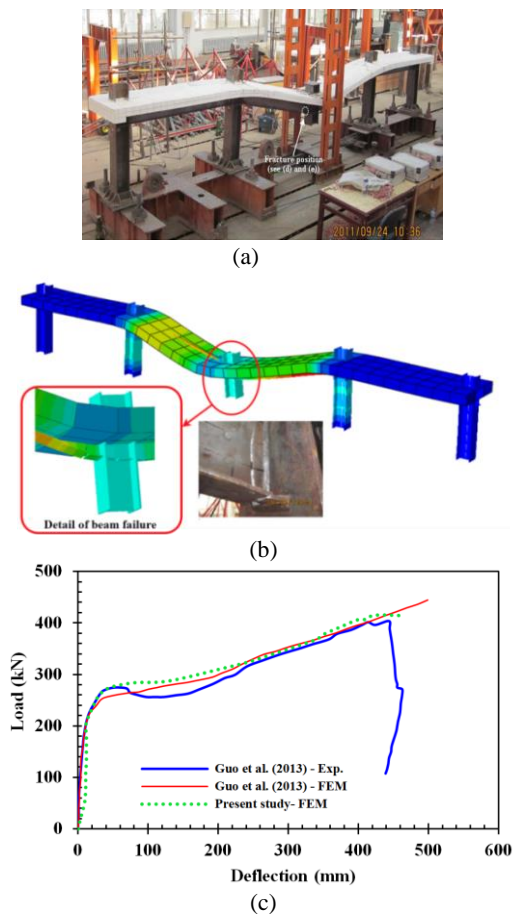


**Figure 9.** Verification of progressive collapse analysis using APM a: Experimental specimen [88] b: FEM in this study c: Comparison of load-displacement diagrams

of Flurat et al. [68] was simulated using the FEM and the technique used in the present study.

In the Flurat et al. [68] study, reinforcement concrete slabs were tested in 3 different modes (Figure 10). Among these models, FS-01-FRP (slab without opening and retrofitted with CFRP) and RLC-02-FRP (slab with opening and retrofitted with CFRP), and RLC-02 (slab with opening and without retrofitting) were selected for validation.

Two of the three selected specimens have CFRP sheets installed using near-surfaces mounted and externally bonded methods. The characteristic compressive strength of the concrete used in the FS-01-(CFRP) and RSC-01 (CFRP) modes was 65 and 62 MPa, respectively. The longitudinal and transverse reinforcing steel were ribbed rebar type. CFRP fibers with a near-surface mounted method have an elastic modulus of 165 GPa and a failure strain of 1.7%. Also, the thickness of the used CFRP sheets is 1.2 mm. Also, CFRP sheets in EBR method had an elastic modulus of 231 GPa and a rupture strain of 1.7%. Also, the thickness of the used CFRP sheets was 0.12 mm. The load was applied incrementally on the upper surface of the reinforcement

concrete slab (center of the slab), and the corresponding displacement was recorded.

Load and displacement values of finite element and laboratory models of FS-01-FRP slabs (slab without opening and retrofitted with CFRP), RLC-02-FRP (retrofitted slab with opening), and RLC-02 (slab with the opening without retrofitting) are shown in Figure 10. As can be seen in this diagram, the maximum load and displacement values obtained from the laboratory specimens and the finite element are close to each other; thus, can say that the finite element simulation method used in the present study can predict the behavior of reinforced concrete slabs reinforced with CFRP sheets with good accuracy. Also, by observing the cracks in slab, the values of the stresses in concrete slab are consistent with the values of the stresses created by the finite element method.

#### 4. 3. Evaluating the Accuracy of the Method used in Simulating Prestressed Slabs

Bailey and Ellobody [69] laboratory study was used to validate the method used in simulating prestressed slabs. Four experiments under heat and two experiments at ambient temperature were performed on strips of prestressed slabs with similar discontinuous tendons. Two post-tensioned slab specimens, T1 and T2, were tested under ambient temperature to determine slab capacity under normal conditions. Four test specimens T1, T2, T3, and T4, were heated using a gas furnace. From these models, T1 model was selected for validation. Post-tensioned concrete slabs were designed by BS 8110-1. The tendons were made of a high-strength 7-strand steel rope. The slabs' length, width, and depth were 4300, 1600, and 160 mm, respectively. The span of the tested slab was 4 m. Each slab had three parabolic tendons with a diameter of 15.7 mm and an area of 150 mm<sup>2</sup>, and average tensile strength of 1846 MPa.

According to Figure 11a, one tendon was placed in the middle of the slab and the other two on both sides at a distance of 530 mm. The two tendon ends were located exactly in the center of the slab depth at the restraint site. The distance between the lower surface of the slab and the tendon center was 37 mm. Steel seats to build the second-degree parabolic path for the tendon were used. Details of the used restraints are shown in Figure 11b. The high compressive strength from the cable to the concrete at the abutment creates tensile stress around the restraints. Other specifications are provided by Bailey and Ellobody [69].

The accuracy of modeling depends on the input data completeness and their precision. The main inputs of this problem include the material's stress-strain curve characteristics. To verify the sample, T1 specimen used. A load-deflection diagram in the middle of the span was obtained and compared with laboratory results. It is impossible to provide a model that exactly matches the experiment results; thus, changing various parameters

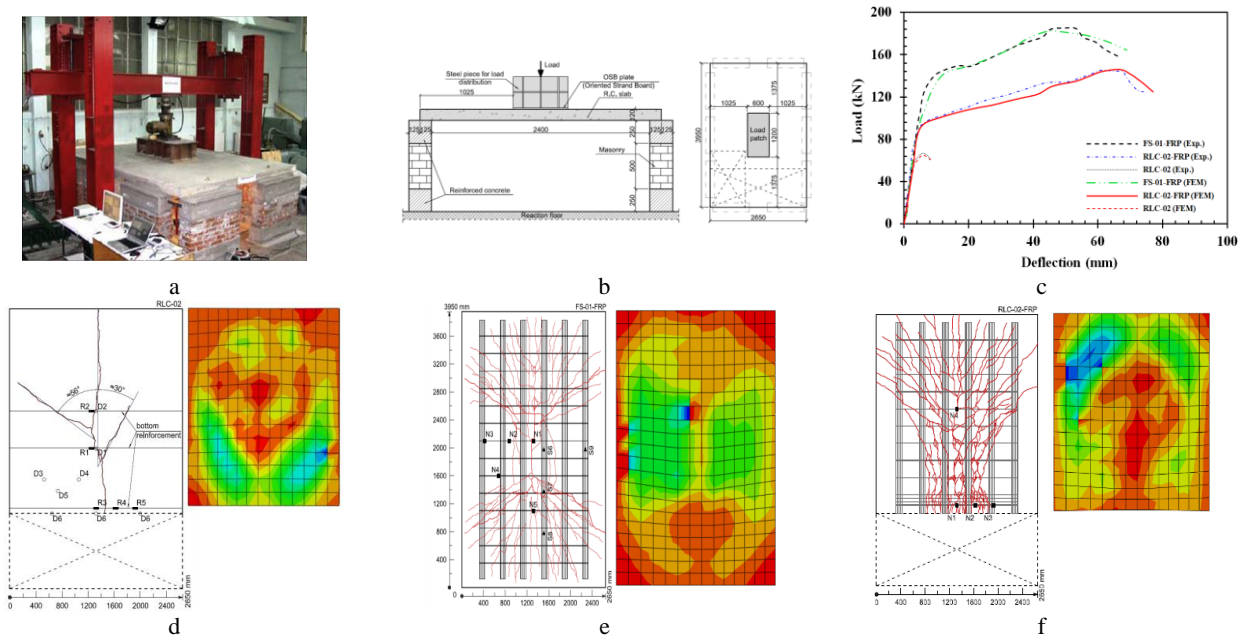


**Figure 10.** Verification of the finite element method used in a simulation of the CFRP sheets on the surfaces of the concrete slabs (a) The slab specimen in the experimental study of Flurat et al.[89] (b) Geometric properties (c) load-deflection curves (d) RLC-02 FEM in this study (e) FS-01-FRP FEM in this study (f) RLC-02-FRP FEM in this study

such as concrete plastic properties, mesh, constraints, boundary conditions, etc., must achieve an acceptable error. Comparison between laboratory and analytical model curves are shown in Figure 11c. The experimental and the numerical achieved ultimate loads were 156.6 kN and 157.3 kN, respectively. The ultimate load predicted by the model has an error of 0.44% compared to the laboratory model and is acceptable with a good approximation.

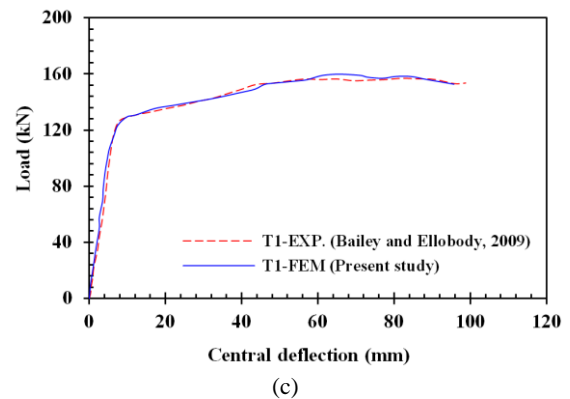
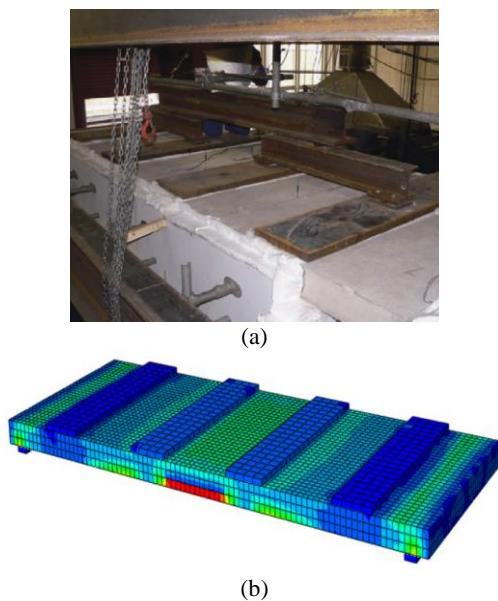


**Figure 11.** (a) Prestressed concrete slabs made in Bailey and Ellobdy [90] laboratory study (b) Displacement contour of finite element model of T1 slab in this study (c) Comparison between the proposed model and laboratory results of load-deflection at ambient temperature



### 5. RESULTS OF COLUMN REMOVAL ANALYSIS

The progressive collapse trend was investigated after modeling and analyzing the buildings. Since all sections were designed to withstand earthquakes and there are no earthquake-related loads in the event of progressive collapse, it is possible that even with the removal of some main load-bearing members; other columns still have sufficient capacity to withstand incoming loads. The outputs for each of the modes are provided below.

**5. 1. Use of Two-way RC Slab as a Floor System**

According to Figure 12, in SMRF buildings with two-way RC slab, two corner columns on the ground floor were removed. The axial force of column B2 in the buildings with a two-way RC slab floor system is shown in Figure 13. The reason for choosing column B2 is that this column is located most adjacent to the removal columns. After the removal process, more axial force is created in it compared to other columns.

When the floor opening is located in the corner of the building plan, and the floor opening dimensions are 4×10 and 6×12 square meters, the axial force of column B2 is equal to 2700 and 2498 kN, respectively. Then over time of analysis, these loads reached 2217 and 2498 kN. The axial forces are created in column B2 when the floor opening is in the middle of the building plan and dimensions are 4×10 and 6×12 square meters, are about 2900 and 3450 kN, respectively, which over time of analysis reduces to 2489 and 2990 kN.

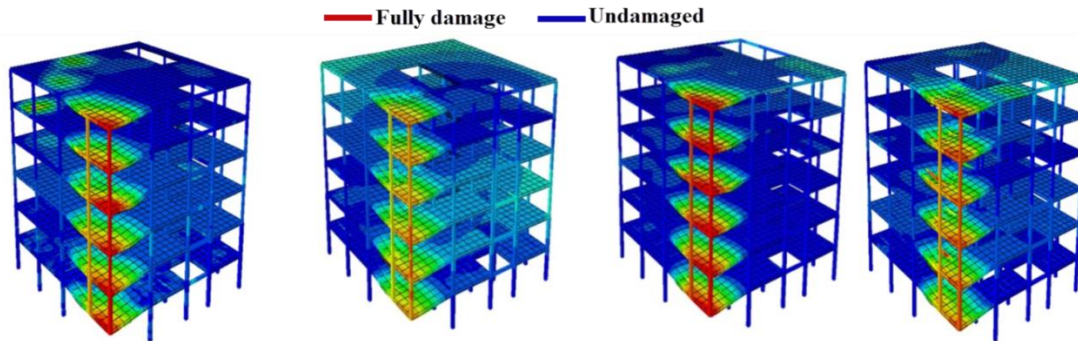
According to the mentioned, it can be stated that in SMRF buildings with two-way RC slab floor system, which is exposed to the removal of corner columns, opening the floor in middle compared to corner, created more axial forces around the removal place. Thus, in a SMRF building with a two-way RC slab where the floor opening is located in the middle compared to the corner, depending on the floor opening dimensions, the axial

forces created around the removed column are more than 18 to 20 percent.

On the other hand, in SMRF buildings with a two-way RC slab floor system, increasing the floor opening dimensions from 4×10 to 6×12 square meters, depending on the floor opening location, the axial force has increased 12 to 19 percent.

The vertical displacement in column removal location is another criterion used to investigate the buildings against progressive collapse. The displacement history of the node above the removed column (column B2) for states 1 to 4 is shown in Figure 14. The largest displacement is related to the case that in the two-way RC slab floor, opening with dimensions of 6×12 square meters is located in the middle of the plan, and its value is 19.3 mm.

Also, the least displacement is related to the situation in the two-way RC slab floor, an opening with dimensions of 4×10 square meters is used in the corner of the plan, and its value is 13.1 mm. According to the obtained displacement values, the choice of floor opening dimensions and location has an impact on the response of steel structures to the removal of the columns; also, the floor opening position has increased the vertical displacement of the node above the removed column by about 25 to 33%, depending on the dimensions of the opening.



Two-way RC slabs- Cor-4×10 Two-way RC slabs-Mid-4×10 Two-way RC slabs- Cor-6×12 Two-way RC slabs-Mid-6×10  
**Figure 12.** Deformed shape in buildings with Two-way RC slabs after removing columns

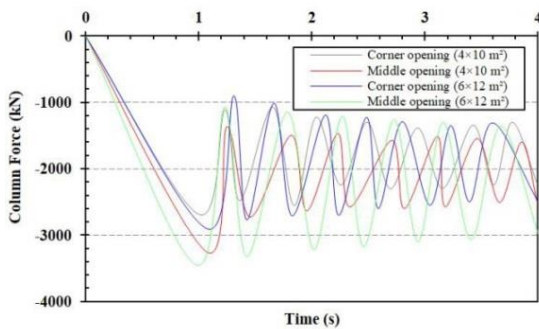


**Figure 13.** The axial force of the column B2 at the ground floor (Two-way RC slab cases)

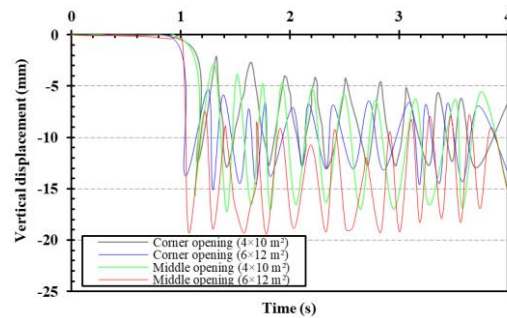
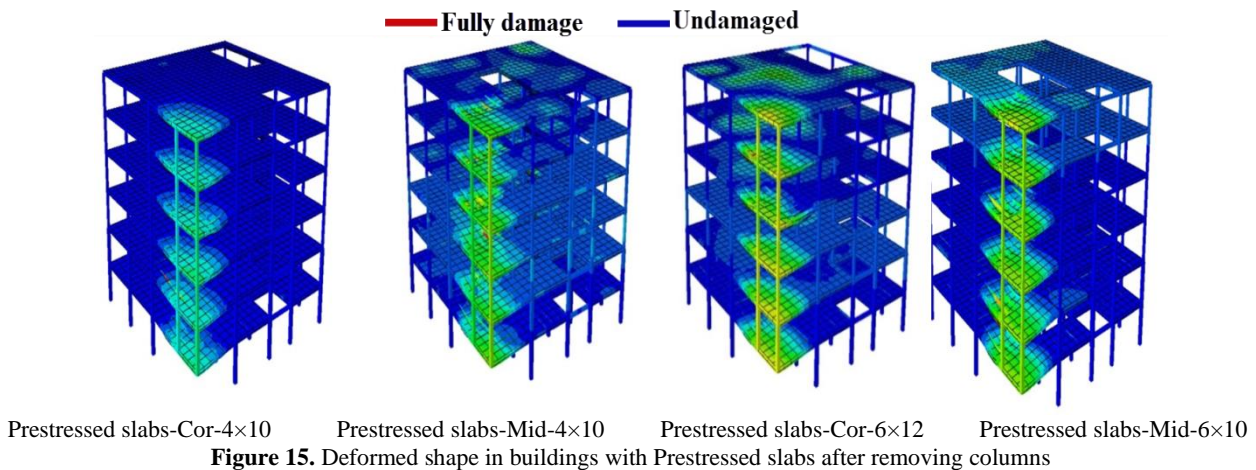


**Figure 14.** Displacement of the node above the removed column (Column A1) for the buildings with two-way RC slab floor systems



### 5. 2. Use of Prestressed Slab System as Floor

Prestressing is necessary to create constant compressive stress in a concrete member. Thus, tensile stresses due to dead and live loads are neutralized in this member due to compressive stress. As a result, load-bearing capacity increases. Permanent compressive stress was applied to the concrete section by completely placing the steel in the concrete part, pulling and restraining it on the member on both sides [70-72]. According to Figure 15, two corner columns on the ground floor were removed in steel buildings with a prestressed slab as the floor system., selected the axial force values of column B2 and the vertical displacement on the removal site.

The axial force of column B2 of SMRF buildings with a prestressed slab system on the floor is shown in Figure 16. The maximum axial force of column B2 for each of the modes PS-slabs-Cor-4x10, PS-Mid-4x10, PS-Cor-6x12, and PS-Mid-6x12, are 1800, 2100, 2100, and 2400 kN, respectively .Changing the floor opening position from the corner to the middle in SMRF buildings with prestressed concrete floor has increased the axial force created around the removal site by 14 to 16 percent, depending on the floor opening dimensions. On the other hand, increasing the floor opening dimensions from 4x10 to 6x12 square meters, depending on the floor opening location, has increased the column adjacent axial force to the removal site by about 15 to 17 percent. The displacement history of the node above the removed column (column B2) for modes 5 to 8 are shown in Figure 17. The maximum displacement is related to the situation that in the prestressed slab floor, an opening with dimensions of 6x12 square meters is installed in the middle of the plan, and its value is equal to 12.3 mm. Also, the least displacement is related to the situation that in the prestressed slab floor, an opening with dimensions of 4x10 square meters is used in the middle of the plan, and its value is equal to 8.1 mm. Changing the prestressed slab opening position from the corner to the middle has

increased the vertical displacement of the node above the removed column from 10 to 30%, depending on the opening dimensions. Also, an 80% increase in the steel building floor opening surface that uses a prestressed slab has increased the vertical displacement depending on opening dimensions of the node above the column by about 16 to 37%.

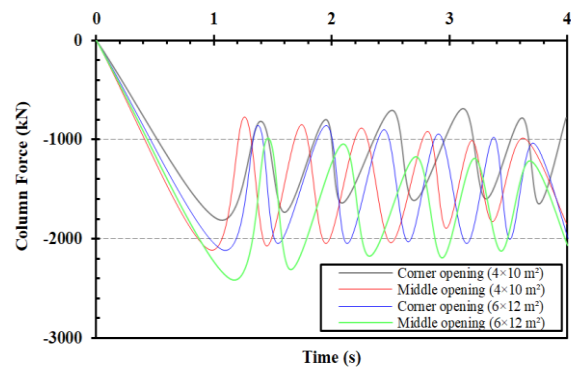


**Figure 16.** The axial force of the column B2 at the ground floor (Prestressed slab cases)

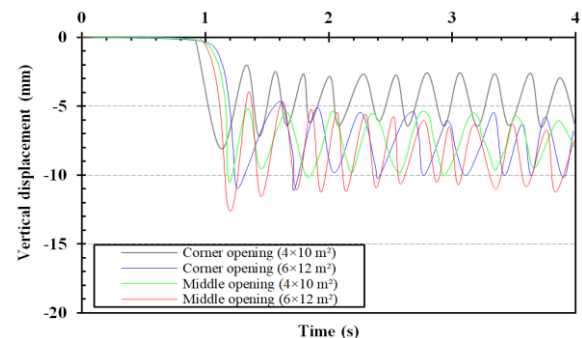


**Figure 17.** Displacement of the node above the removed column (Column A1) for the buildings with prestressed slab floor

**5. 3. Use of Two-way RC Slab System Retrofitted with CFRP Sheets**

Retrofitting concrete slab with CFRP is done locally to increase the bearing capacity of the slab, increase the slab resistance to corrosion, decrease compressive strength of concrete, increase flexural strength, shear, etc. Slabs are responsible for withstanding vertical loads, but because they also have the function of the horizontal diaphragm, they must be connected to the structure's strong lateral members and have sufficient rigidity and strength. A concrete slab retrofitted with CFRP can increase bending capacity. This method can also restore the original capacity of the slab, which has been reduced due to steel corrosion. Today, fiber-reinforced polymeric materials instead of traditional materials and existing methods are common in the world. Retrofitted slab with CFRP, while having lightweight, has high tensile strength [73-76].

Following Figure 18, in steel buildings with two-way RC slab floors retrofitted with CFRP sheets, removed two corner columns were on the ground floor. In this case, the axial force of column B2 and vertical displacement in the removal location were extracted. The axial force of column B2 in SMRF buildings with

retrofitted two-way RC slabs (CFRP sheets) is shown in Figure 19. The maximum axial force of modes CFRP-Cor-4×10, CFRP-Mid-4×10, CFRP-Cor-6×12, and CFRP-Mid-6×12 is 2580, 2750, 2700, and 2900 kN, respectively.

In SMRF buildings with retrofitted two-way RC slab using CFRP, changing the floor opening position from the corner to the middle depending on the floor opening dimensions increased the axial force created around the removal site by 6.5 up to 7%. On the other hand, increasing the floor opening dimensions from 4×10 to 6×12 square meters, depending on the floor opening location, has increased the axial force of the column adjacent to the removal site by about 4 to 7.5 percent. The displacement history of the node above the removal column (column B2) for states 9 to 12 are shown in Figure 20. An 80% increase in the floor opening dimensions located in the middle of the plan has increased the displacement of the removal site to the 14 to 46%, depending on the floor opening position. In terms of the removal column location displacement, it is better to place the floor opening in the corner of the plan than

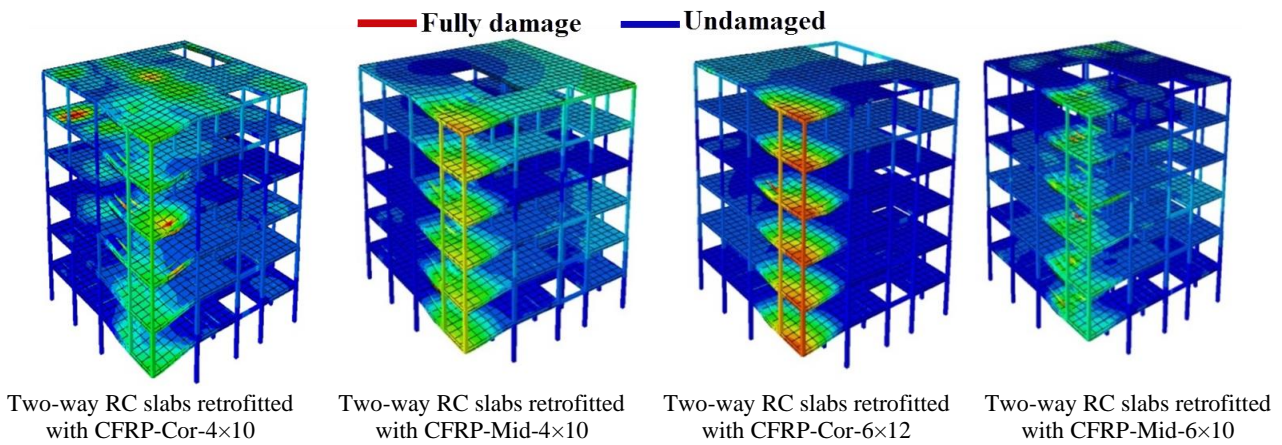


**Figure 18.** Deformed shape in buildings with Two-way RC slabs after removing columns

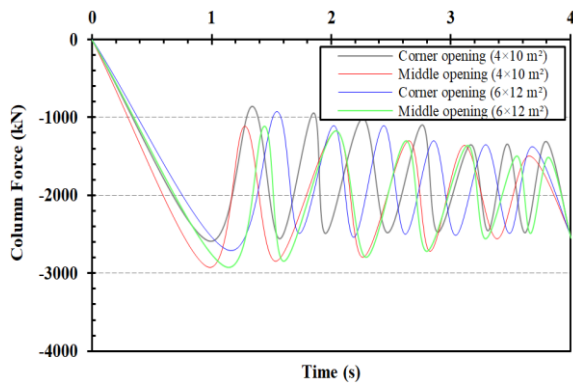


**Figure 19.** The axial force of the column B2 at the ground floor (two-way RC slabs retrofitted with CFRP cases)

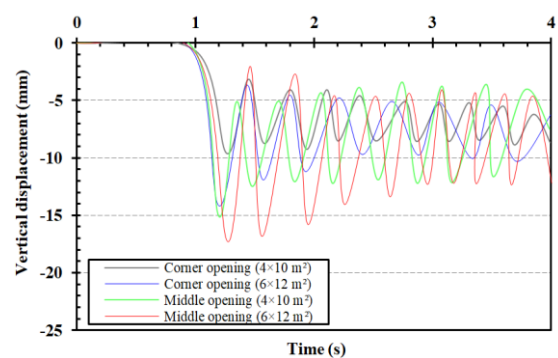


**Figure 20.** Displacement of the node above the removed column (Column A1) for the buildings with two-way RC slabs retrofitted with CFRP cases

to place it in the middle of the building plan; Because the displacement corresponding to the floor opening positions in the middle, depending on the floor opening dimensions, is 56 to 46 percent higher than the values corresponding to the floor opening position in the corner.

## 6. RESULTS

Progressive collapse analysis of buildings without considering the floor simulation can affect the engineering judgment about the strength of a structure [19]. One of the studied variable parameters is the effect of floor type on the SMRF buildings against column removal. In the present study, three types of conditions were for the building floor, including two-way RC slabs, prestressed slab, and two-way RC slab retrofitted with CFRP sheets, respectively. The maximum axial force created in the column adjacent to the removal site on the ground floor for the 12 modes is presented in Figure 21. The best performance in axial force redistribution is related to the buildings in which the prestressed slab is used as a gravity bearing system. The corresponding axial forces of the PS-Cor-4×10, PS-Mid-4×10, PS-Cor-6×12, and PS-Mid-6×12 modes are 33, 35, 27, and 30% less than corresponding values in buildings with two-way RC slab, respectively.

The low tensile strength of concrete and vulnerability are major problems in the concrete components. On the other hand, concrete is very resistant to pressure. Also, after bending due to the application of load, it remains under pressure by pre-compression of the concrete member, thus providing a more efficient design. Therefore, the present study analysis results confirm that prestressed concrete slabs have higher yield strength and over-strength due to prestressed tendons than conventional steel reinforcement. The basic design criterion of RC for both prestressed and non-prestressed types is to place steel reinforcement in the positions of the concrete that will be created by external loading. In prestressed concrete, high-strength steel rebar is used, which is pulled before applying external load. This initial tension of the steel rebar pre-compressed the adjacent concrete and created a condition in which the concrete can undergo more loads before cracking. In non-prestressed slabs, there is no stress or strain in either steel or concrete before applying loads. It requires a relatively small load for creating cracks on concrete on such a floor. The tensile stresses created in the steel rebar of the floor slab are very small before cracking.

During the failure, the moment is tolerated by creating high tensile stresses in the reinforcement bar and high compressive stresses in concrete. The action of prestressing creates a self-balancing stress system. These self-balancing stresses are high tensile stresses in prestressed steel that result in a tensile force  $P$  and cross-tensions in concrete that results in a compressive force

equal to  $P$ .

The axial force corresponding to CFRP-Cor-4×10, CFRP-Mid-4 × 10, CFRP-Cor-6 × 12, and CFRP-Mid-6×12 modes are 4, 15, 7, and 16% less than corresponding values in buildings with two-way RC slabs, respectively. The maximum vertical displacement of the column removal location for the 12 modes is shown in Figure 22.

The displacement corresponding to the buildings, in which the prestressed slab is used, depending on the location of the floor opening and the dimensions of the opening, is about 27 to 39 percent less than the values corresponding to the buildings with two-way RC slabs.

The use of prestressed cables on the floor effectively reduces the structure's potential against progressive collapse and can reduce the moment in the critical section and increase the bearing capacity. Also, the corresponding displacement of buildings that use reinforcement two-way RC slab with CFRP, depending on the floor opening location and the floor opening dimensions, is about 8 to 26 percent less than the values corresponding to buildings with two-way RC slabs. Investigating the deformation condition and stress contours in the structures after removing the two

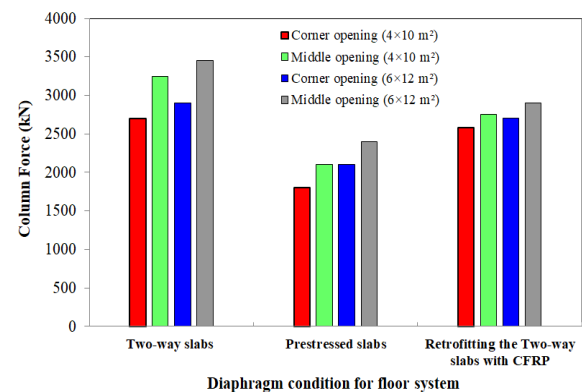


Figure 21. Comparison of the maximum Axial force of column B2 at the ground floor

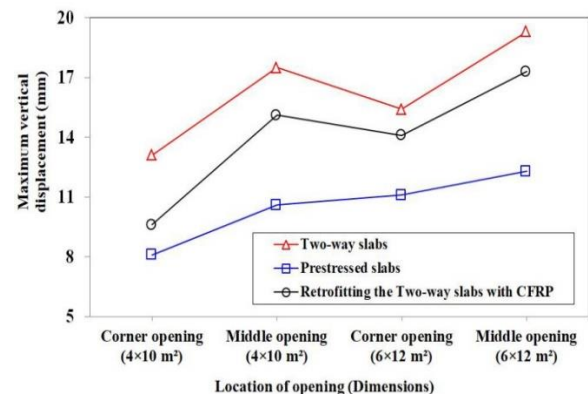


Figure 22. Comparison of the maximum vertical displacement of the node above column A1

corner columns can say that the structure's deformation occurs locally in the same corner panel. The rest of the structure remains integrated and elastic. The diagrams related to the axial force in the columns adjacent to the removal corner column in the structural model found that the most effective after removing the corner column is on column B2.

By observing the flexural condition of beams and connections in the damaged area for structures can be expressed, all beams are designed with sufficient flexural strength and stiffness; even after removing two key columns from the structure, can withstand the spread of collapse. However, in the case of flexural connections, it should be noted that connections usually have less rotational capacity than members of structures such as beams. Thus, to prevent the spread of damage in the structure after column removal, it is necessary to use bending connections with more ductility due to having more rotational capacity. If the vertical deformation of the structure increases after column removal, it can absorb and depreciate by enduring longer periods and provide more energy to the structure.

According to the displacement diagram and the flexural moment near and far from the failure point in the corner column, using prestressed slabs and CFRP sheets can reduce the amount of deflection and flexural moment.

Regarding the displacement of the top point of the removal column and flexural moment in the position near and far from the failure point in the corner column, using prestressed slabs and CFRP sheets can reduce the deflection and flexural moment. Because columns in steel-moment frames are primarily responsible for providing lateral stiffness, they usually have sufficient size and strength. Accordingly, by increasing the ductility due to the selection of sections based on compression constraints commensurate with the desired ductility, the column's performance against the spread of collapse improves. Control of member deformation criteria is one of the acceptance criteria that should be considered in evaluating the structure's behavior against progressive collapse. Deformation limits are applied to ensure a proper response to column removal.

In the structure design, the stresses created in the members are compared and controlled with the allowable stresses. But in the design against the progressive collapse the deformation, is the basis for judging the structure acceptability based on performance levels. These limits are determined based on laboratory results or experimental evidence. Because loads from accidents such as explosions, design errors, execution, impact, etc., are unpredictable, a conservative amount is considered to ensure sufficient section capacity. Limitations for deformation are determined based on safety concepts and protection criteria on the building performance levels.

One of these limitations is the rotation criterion, which makes the maximum deformation response a

function of the member length and indicates the percentage of instability in the critical areas of the member. The rotation of beams and columns is calculated according to GSA [2] using Equations (7) and (8). The parameter  $\theta$  is shown in Figure 23.

$$\theta = \frac{ZF_{ye}L_b}{6EI_b} \quad (7)$$

$$\theta = \frac{ZF_{ye}L_c}{6EI_c} \left(1 - \frac{P}{P_{ye}}\right) \quad (8)$$

where  $Z$  = Plastic section modulus,  $F_{ye}$  = Expected yield strength of the material,  $I$  = moment of inertia,  $L_b$  = Beam length,  $L_c$  = Column length,  $E$  = Modulus of elasticity,  $P$  = Axial force in the member,  $P_{ye}$  = Expected axial yield force of the member.

The maximum rotation angles of the beams and columns for the 12 cases are shown in Figures 24 and 25. In these figures, the allowable rotation angle according to the GSA regulations is shown. According to GSA, the maximum rotation angle of beams and columns is 0.21 radians. In the mentioned figures, the values of the maximum rotation angle with the regulations allowable value are also compared with each other. The maximum rotation angle of the beams in the cases corresponding to the concrete slabs is more than 0.21 radians. The maximum rotation angle of the beams corresponding to the modes S-C-4×10, S-C-6×10, S-M-4×10, and S-M-6×12 has been 0.26, 0.3, 0.28, and 0.31 radians, respectively.

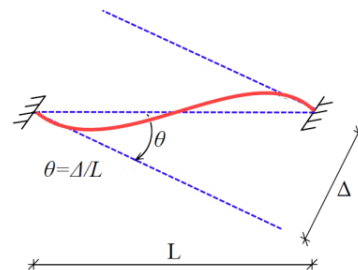


Figure 23. Definition of chord rotation [2]

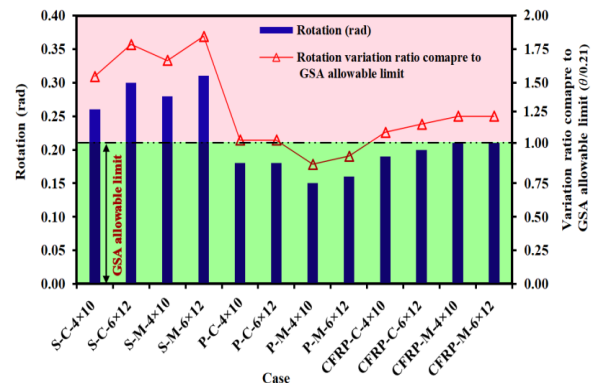
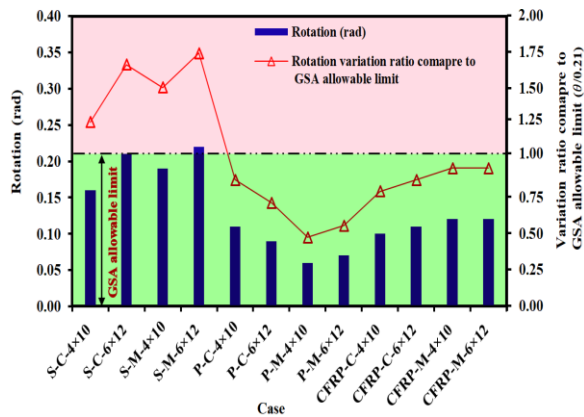


Figure 24. Maximum angle rotation of the beams and their comparison with the allowable value of GSA regulations



**Figure 25.** Maximum angle rotation of the columns and their comparison with the allowable value of GSA regulations

The use of prestressed concrete slabs has significantly reduced the beam's rotation angle. The rotation angles corresponding to the modes P-C-4×10, P-C-6×10, P-M-4×10, and P-M-6×12 have been 0.18, 0.18, 0.15, and 0.16 radians, respectively. This means that the maximum angle rotation corresponding to the retrofitted states with prestressed slabs, depending on the floor opening dimensions and position, is 31 to 48% lower than the values corresponding to two-way RC slabs mode. The cables used to prestress the concrete slabs increased the energy absorption behavior of the structure against column removal by increasing energy absorption, and the beams and columns around the removal site performed better in redistributing forces. On the other hand, the maximum beam rotation angles corresponding to CFRP-C-4×10, CFRP-C-6×10, CFRP-M-4×10, and CFRP-M-6×12 modes have been 0.19, 0.2, 0.21, and 0.21, respectively. The addition of CFRP sheets to the exterior surfaces of two-way RC slabs has reduced the maximum rotation angle of the beams adjacent to the removal location by 25 to 33%, depending on the floor opening position and dimensions.

The maximum angle rotation of the columns is shown in Figure 25 and compares with the GSA limit. The maximum angle rotation of the columns corresponding to the modes S-C-4×10, S-C-6×10, S-M-4×10, and S-M-6×12 has been 0.16, 0.21, 0.19, and 0.22, respectively.

The rotational angles corresponding to the modes P-C-4×10, P-C-6×10, P-M-4×10, and P-M-6×12 were 0.11, 0.09, 0.06, and 0.07, respectively. This means that the maximum angle rotation of the columns corresponding to the modes of use of prestressed slabs, depending on the floor opening dimensions and position, is 31 to 68% less than the values corresponding to the conventional two-way RC slabs mode. The compressive force applied to the concrete due to prestressing will neutralize the tensile stress due to the applied loads. The whole member will pressurize, and carry the compressive force by the concrete will be used optimally. On the other hand, due to the removal of tensile stress and the placement of the

entire section in compression, the need for rebar in a concrete member similar to an RC member is reduced. Also, the member's behavior in the bent position is improved, and the tensile cracks are removed, and the deformation is reduced. As a result, the main purpose of prestressing a concrete member is to limit the tensile stresses and cracks caused by the bending moment due to the loads applied to that member, and this process leads to an improvement in the response of the structure against progressive failure. On the other hand, the maximum rotation angles of the columns corresponding to CFRP-C-4×10, CFRP-C-6×10, CFRP-M-4×10, and CFRP-M-6×12 have been 0.1, 0.11, 0.12, and 0.12, respectively. The addition of CFRP sheets to the exterior surfaces of two-way RC slabs has reduced the maximum rotation angle of adjacent columns to the removal location by 36 to 47%, depending on the location and floor opening dimensions.

## 7. SUMMARY AND CONCLUSIONS

Due to the removal of large amounts of concrete and reinforcement bars, the ability of the structure to withstand the loads may be reduced, and there may be a need to provide a solution to increase the load-bearing capacity.

This study investigated another method to increase the bearing capacity of the structure called prestressing and evaluated the effect of the surface and position of the RC floor opening on the progressive collapse potential of SMRF buildings. Proposed two solutions to rehabilitate and retrofit two-way RC slabs against progressive collapse. To rehabilitate, prestressed RC slabs were used, and to retrofit, used the method of installing CFRP sheets on the surface of the old concrete slab. In this section, the most important results are presented:

- The use of cable systems to restore the cross-section to its original shape is suitable for repair and can reduce the flexural moment in the critical section and increase the bearing capacity. The displacement corresponding to the buildings, in which the prestressed slab is used, depending on the opening and the dimensions of the opening, is about 27% to 39% less than the values corresponding to the buildings with two-way RC slabs. The use of prestressed cables in the roof effectively reduces the potential of the structure against progressive collapse.
- In SMRF buildings with a two-way RC slab system that is exposed to the removal of corner columns, the presence of an opening in the middle of the building plan creates more axial forces around the removal site compared to the position in which the floor opening is in the corner of the plan. Also, the axial forces created around the removed column of the SMRF buildings with a two-way slab in which the opening is located in the middle of the plan, depending on the

opening dimensions, is about 18% to 20% more than the corresponding value in the presence of an opening in the corner.

- In SMRF buildings with a two-way RC slab floor system, increasing the opening ranges from 4×10 square meters to 6×12 square meters, depending on the location of the opening, has increased the axial force created around the removal site by about 12% to 19%. Changing the opening from the corner to the middle in SMRF buildings with prestressed concrete slabs has increased the axial force created around the removal site by 14% to 16 %, depending on the dimensions of the opening. On the other hand, increasing the dimensions of the opening from 4×10 to 6×12 square meters, depending on the location of the opening, has increased the axial force of the column adjacent to the removal site by about 15% to 17%. According to the obtained displacement values, it can be stated that the choice of dimensions and location of the opening has an impact on the response of SMRF buildings to column removal; an 80% increase in the floor opening surface in a steel structure using a two-way RC slab has increased the vertical displacement of the node above the column by about 10% to 17%, depending on the floor opening position.
- Retrofitting of concrete slab with CFRP is done locally to increase the bearing capacity of the slab, increase the slab resistance to corrosion, and increase flexural and shear strength. Slabs are practically responsible for withstanding vertical loads. Because they also have the function of the horizontal diaphragm, they must be connected to the strong lateral members of the structure and have sufficient rigidity and strength. This method can also restore the original capacity of the slab, which has been reduced due to corrosion of the steel.

## 8. REFERENCES

1. UFC 4-023-03, "Design of Buildings to Resist Progressive Collapse." Department of Defense Unified Facilities Criteria, (2016).
2. GSA, General Service Administration, Washington D.C "Alternate path analysis and design guidelines for progressive collapse resistance", (2016).
3. ASCE 7-05, "Minimum Design Loads for Buildings and Other Structures". American Society of Civil Engineers New York, (2005).
4. Kiakojouri, F., De Biagi, V., Chiaia, B., Sheidaii, M. R. (2020). "Progressive collapse of framed building structures: Current knowledge and future prospects." *Engineering Structures*, (2020), Vol. 206, 110061, DOI: 10.1016/j.engstruct.2019.110061
5. Galal, M. A., Bandyopadhyay, M., Banik, A. K. "Dual effect of axial tension force developed in catenary action during progressive collapse of 3D composite semi-rigid jointed frames." *Structures*, Vol. 19, (2019), 507-519.
6. Shakib, H., Zakersalehi, M., Jahangiri, V., Zamanian, R. "Evaluation of plasco building fire-induced progressive collapse." *Structures*, Vol. 28, (2020), 205-224, DOI: 10.1016/j.istruc.2020.08.058.
7. Bagheripourasil, M., Mohammadi, Y. "Comparison between alternative load path method and a direct applying blast loading method in assessment of the progressive collapse;" *Journal of Rehabilitation in Civil Engineering*, Vol. 3, No. 2, (2015), 1-15, DOI: 10.22075/jrce.2015.367.
8. Pourasil, M.B., Mohammadi, Y. Gholizad, A. "A proposed procedure for progressive collapse analysis of common steel building structures to blast loading." *KSCSE Journal of Civil Engineering*, Vol. 21, (2017), 2186-2194, DOI: 10.1007/s12205-017-0559-0
9. Abdelwahed, B. "A review on building progressive collapse, survey and discussion" *Case Studies in Construction Materials*, Vol. 11, e00264 DOI: 10.1016/j.cscm.2019.e00264
10. Fruhwald, E., Serrano, E., Toratti, T., Emilsson, A., Thelandersson, S. "Design of safe timber structures-How can we learn from failures in concrete, steel and timber?"; Report TVBK-3053, 2007.
11. Russell, J. M., Sagaseta, J., Cormie, D., Jones, A. E. K. "Historical review of prescriptive design rules for robustness after the collapse of Ronan Point." *Structures*, Vol. 20, (2019), 365-373.
12. Byfield, M., Mudalige, W., Morison, C., Stoddart, E. "A review of progressive collapse research and regulations." *Proceedings of the Institution of Civil Engineers-Structures and Buildings*, Vol. 167, No. 8, (2014), 447-456, DOI: 10.1680/stbu.12.00023.
13. Martin, R., Delatte, N. J. "Another looks at the L'Ambiance Plaza collapse." *Journal of Performance of Constructed Facilities*," Vol. 14, No. 4, (2000), 160-165, DOI: 10.1061/(ASCE)0887-3828(2000)14:4(160)
14. Osteraas, J. D. "Murrah building bombing revisited: A qualitative assessment of blast damage and collapse patterns." *Journal of Performance of Constructed Facilities*, Vol. 20, No. 4, (2006), 330-335, DOI: 10.1061/(ASCE)0887-3828(2006)20:4(330).
15. Gardner, N. J., Huh, J., Chung, L. "Lessons from the Sampoong department store collapse." *Cement and Concrete Composites*, Vol. 24, No. 6, (2002), 523-529. DOI: 10.1016/S0958-9465(01)00068-3.
16. El-Tawil, S., Li, H., Kunnath, S. "Computational simulation of gravity-induced progressive collapse of steel-frame buildings: Current trends and future research needs." *Journal of Structural Engineering*, Vol. 140, No. 8, (2014), A2513001, DOI: 10.1061/(ASCE)ST.1943-541X.0000897.
17. Kotsovinos, P., Usmani, A. "The World Trade Center 9/11 disaster and progressive collapse of tall buildings." *Fire Technology*, Vol. 49, No. 3, (2013), 741-765, DOI: 10.1007/s10694-012-0283-8.
18. Bosela Jr, P., Bosela, P. "Tropicana Parking Garage Collapse." In *Forensic Engineering 2018: Forging Forensic Frontiers* Reston, VA: American Society of Civil Engineers. (2018), 1118-1124.
19. Kaafi, P., Ghodrati Amiri, G. "Investigation of the progressive collapse potential in steel buildings with composite floor system," *World Academy of Science, Engineering and Technology, International Journal of Civil and Environmental Engineering*, Vol.1, No. 8, (2014).
20. Maqsood, S. T., Schwarz, J. "Analysis of building damage during the 8 October 2005 earthquake in Pakistan." *Seismological Research Letters*, Vol. 79, No. 2, (2008), 163-177, DOI: 10.1785/gssrl.79.2.163
21. Rigby, S. E., Lodge, T. J., Alotaibi, S., Barr, A. D., Clarke, S. D., Langdon, G. S., Tyas, A. "Preliminary yield estimation of the 2020 Beirut explosion using video footage from social media" *Shock Waves*, (2020), 1-5.

22. Mousapoor, E., Ghiyasi, V., Madandoust, R. "Macro modeling of slab-column connections in progressive collapse with post-punching effect." *Structures*, Vol. 27, (2020), 837-852, DOI: 10.1016/j.istruc.2020.06.025.
23. Shan, S., Li, S. "Fire-induced progressive collapse mechanisms of steel frames with partial infill walls", *Structures*, Vol. 25, (2020) 347-359, DOI: 10.1016/j.istruc.2020.03.023.
24. Meng, B., Hao, J., Zhong, W., Tan, Z., Duan, S. "Improving collapse-resistance performance of steel frame with openings in beam web." *Structures*, Vol. 27, 2156-2169, DOI: 10.1016/j.istruc.2020.08.009.
25. Rezvani, F. H., Yousefi, A. M., Ronagh, H. R. "Effect of span length on progressive collapse behaviour of steel moment resisting frames." *Structures*, Vol. 3, 81-89, DOI: 10.1016/j.istruc.2015.03.004.
26. Kong, D. Y., Yang, Y., Yang, B., Zhou, X. H. "Experimental Study on Progressive Collapse of 3D Steel Frames under Concentrated and Uniformly Distributed Loading Conditions." *Journal of Structural Engineering*, Vol. 146, No. 4, (2020), 04020017.
27. Wang, J., Wang, W., Bao, Y., Lehman, D. "Numerical investigation on progressive collapse resistance of steel-concrete composite floor systems." *Structure and Infrastructure Engineering*, (2020), Vol. 18, No. 2, 1-15, DOI: 10.1080/15732479.2020.1733622
28. Tavakoli, H. R., Alashti, A. R. "Evaluation of progressive collapse potential of multi-story moment resisting steel frame buildings under lateral loading", *Scientia Iranica*, Vol. 20, No. 1, (2013), 77-86.
29. Wang, W. M., Li, H. N., Tian, L. "Progressive collapse analysis of transmission tower-line system under earthquake." *Advanced Steel Construction*, Vol. 9, No. 2, (2013), 161-172.
30. Salmasi, A. C., Sheidaii, M. R. "Assessment of eccentrically braced frames strength against progressive collapse." *International Journal of Steel Structures*, Vol. 17, No. 2, 543-551.
31. Qiao, H., Luo, C., Wei, J., Chen, Y. "Progressive Collapse Analysis for Steel-Braced Frames Considering Vierendeel Action." *Journal of Performance of Constructed Facilities*, Vol. 34, No. 4, (2020), 04020069.
32. Elsanadedy, H. M., Al-Salloum, Y. A., Alrubaidi, M. A., Almusallam, T. H., Abbas, H. "Finite element analysis for progressive collapse potential of precast concrete beam-to-column connections strengthened with steel plates, *Journal of Building Engineering*, Vol. 34, No. 11, (2020), 101875, DOI: 10.1016/j.jobe.2020.101875
33. Sun, R., Huang, Z., Burgess, I. W. "Progressive collapse analysis of steel structures under fire conditions." *Engineering Structures*, Vol. 34, (2012), 400-413, DOI: 10.1016/j.engstruct.2011.10.009.
34. Gerasimidis, S., Sideri, J. "A new partial-distributed damage method for progressive collapse analysis of steel frames." *Journal of Constructional Steel Research*, Vol. 119, (2016), 233-245. DOI: 10.1016/j.jcsr.2015.12.012
35. Pordel Maragheh, B., Jalali, A., Mirhoseini Hezaveh, S. M. (2020). "Effect of Initial Local Failure Type on Steel Braced Frame Buildings against Progressive Collapse." *International Journal of Engineering, Transactions A: Basics*, Vol. 33, No. 1, (2020), 34-46. doi: 10.5829/ije.2020.33.01a.05
36. Fu, F., "3-D nonlinear dynamic progressive collapse analysis of multi-story steel composite frame buildings—Parametric study." *Engineering Structures*, Vol. 32, No. 12, (2010), 3974-3980, DOI: 10.1016/j.engstruct.2010.09.008.
37. Naji, A., Irani, F. "Progressive collapse analysis of steel frames: Simplified procedure and explicit expression for dynamic increase factor." *International Journal of Steel Structures*, Vol. 12, No. 4, (2012), 537-549.
38. Karimian, A., Armaghani, A., Behravesht, A. "Performance of Low-yield Strength Plates in Beam-column Connections against Progressive Collapse." *KSCCE Journal of Civil Engineering*, Vol. 23, No. 1, (2019), 335-345, DOI: 10.1007/s12205-018-0653-y
39. Zahrai, S. M., Zeighami, E. "Cyclic Behavior of Various Drilled Flange Beam Connected to Box Column." *AUT Journal of Civil Engineering*. DOI: 10.22060/ajce.2020.17448.5633
40. Liu, C., Fung, T. C., Tan, K. H. "Dynamic performance of flush end-plate beam-column connections and design applications in progressive collapse." *Journal of Structural Engineering*, Vol. 142, No. 1, (2016), 04015074, DOI: 10.1061/(ASCE)ST.1943-541X.0001329
41. Yang, B., Tan, K. H. "Robustness of bolted-angle connections against progressive collapse: Experimental tests of beam-column joints and development of component-based models." *Journal of Structural Engineering*, Vol. 13, No. 9, (2013) 1498-1514, DOI: 10.1061/(ASCE)ST.1943-541X.0000749
42. Wang, F., Yang, J., Pan, Z. "Progressive collapse behaviour of steel framed substructures with various beam-column connections." *Engineering Failure Analysis*, Vol. 109, (2020), 104399, DOI: 10.1016/j.engfailanal.2020.104399
43. Chen, Y., Huo, J., Chen, W., Hao, H., Elghazouli, A. Y. "Experimental and numerical assessment of welded steel beam-column connections under impact loading." *Journal of Constructional Steel Research*, Vol. 175, (2020), 106368, DOI: 10.1016/j.jcsr.2020.106368.
44. Li, S. Q., Yu, T. L., Jia, J. F. "Empirical seismic vulnerability and damage of bottom frame seismic wall masonry structure: A case study in Duijiangyan (China) region", *International Journal of Engineering, Transactions C: Aspects*, Vol. 32, No. 9, (2019), 1260-1268. DOI: 10.5829/ije.2019.32.09c.05.
45. Li, S. Q., Yu, T. L., Jia, J. F. "Investigation and analysis of empirical field seismic damage to bottom frame seismic wall masonry structure", *International Journal of Engineering, Transactions B: Applications*, Vol. 32, No. 8, (2019), 1082-1089. DOI: 10.5829/ije.2019.32.08b.04
46. Li, S. Q., Yu, T. L., Chen, Y. S. "Comparison of macroseismic intensity scales by considering empirical observations of structural seismic damage", *Earthquake Spectra*, Vol. 37, No. 1, (2021), 449-485. DOI: 10.1177/8755293020944174
47. Ozturk, B., Yilmaz, C., Şentürk, T. "Effect of FRP retrofitting application on seismic behavior of a historical building at Niğde", 14th European Conference on Earthquake Engineering 2010: Ohrid, Republic of Macedonia, (2010).
48. Ozturk, B. "Seismic behavior of two monumental buildings in historical Cappadocia region of Turkey." *Bulletin of Earthquake Engineering*, Vol. 15, No. 7, (2017), 3103-3123.
49. Oztürk, B., Şentürk, T., Yilmaz, C. "Analytical Investigation of Effect of Retrofit Application using FRP on Seismic Behavior of a Monumental Building at Historical Cappadocia Region of Turkey."
50. Zhu, Y. F., Chen, C. H., Huang, Y., Huang, Z. H., Yao, Y., Keer, L. M. "Dynamic progressive collapse of steel moment frames under different fire scenarios." *Journal of Constructional Steel Research*, Vol. 173, (2020), 106256.
51. Wang, F., Yang, J., Pan, Z. "Progressive collapse behaviour of steel framed substructures with various beam-column connections." *Engineering Failure Analysis*, Vol. 109, (2020), 104399, DOI: 10.1016/j.engfailanal.2020.104399.
52. Qiao, H., Chen, Y., Wang, J., Chen, C. "Experimental study on beam-to-column connections with reduced beam section against progressive collapse." *Journal of Constructional Steel Research*, Vol. 175, (2020), 106358, DOI: 10.1016/j.jcsr.2020.106358.

53. Mousapoor, E., Ghiyasi, V., Madandoust, R. "Macro modeling of slab-column connections in progressive collapse with post-punching effect." *Structures*, Vol. 27, 837-852, DOI: 10.1016/j.istruc.2020.06.025.
54. Livingston, E., Sasani, M., Bazan, M., Sagiroglu, S. "Progressive collapse resistance of RC beams." *Engineering Structures*, Vol. 95, (2015), 61-70, DOI: 10.1016/j.engstruct.2015.03.044
55. Abaqus theory manual. Version, Hibbitt. (2016). Pawtucket (RI): Karlsson and Sorensen, Inc.
56. Torabian, A., Isufi, B., Mostofinejad, D., Ramos, A. P. "Flexural strengthening of flat slabs with FRP composites using EBR and EBROG methods." *Engineering Structures*, Vol. 211, (2020), 110483.
57. Sharif, A., Al-Sulaimani, G. J., Basunbul, I. A., Baluch, M. H., Ghaleb, B. N. "Strengthening of initially loaded reinforced concrete beams using FRP plates." *Structural Journal*, Vol. 91, No. 2, (1994), 160-168.
58. Mostofinejad, D., Hajrasouliha, M. "Shear retrofitting of corner 3D-reinforced concrete beam-column joints using externally bonded CFRP reinforcement on grooves." *Journal of Composites for Construction*, Vol. 22, No. 5, (2018), 04018037, DOI: 10.1061/(ASCE)CC.1943-5614.0000862.
59. Jafarian, N., Mostofinejad, D., Naderi, A. "Effects of FRP grids on punching shear behavior of reinforced concrete slabs." *Structures*, Vol. 28, 2523-2536, DOI: 10.1016/j.istruc.2020.10.061
60. Gao, D., Fang, D., You, P., Chen, G., Tang, J. "Flexural behavior of reinforced concrete one-way slabs strengthened via external post-tensioned FRP tendons." *Engineering Structures*, Vol. 216, (2020), 110718, DOI: 10.1016/j.engstruct.2020.110718.
61. Chen, W., Pham, T. M., Elchalakani, M., Li, H., Hao, H., Chen, L. "Experimental and Numerical Study of Basalt FRP Strip Strengthened RC Slabs under Impact Loads." *International Journal of Structural Stability and Dynamics*, Vol. 20, No. 6, (2020), 2040001, DOI: 10.1142/S0219455420400015.
62. Tao, Y., Wang, W. "Flexural performance of Reinforced Concrete One-way Slabs Strengthened by FRP Grid." *In IOP Conference Series: Earth and Environmental Science*, Vol. 560, No. 1, 012092, IOP Publishing.
63. ETABS, C. (2015). 15.0. Berkeley. CA: Computers and Structures Inc.
64. Feng Fu. "Response of a multi-storey steel composite building with concentric bracing under consecutive column removal scenarios." *Journal of Constructional Steel Research*, Vol. 70, (2012), 115-126. DOI: org/10.1016/j.jcsr.2011.10.012.
65. Hosseini, S. M., Amiri, G. G. "Successive collapse potential of eccentric braced frames in comparison with buckling-restrained braces in eccentric configurations" *International Journal of Steel Structures*, Vol. 17, No. 2, (2017), 481-489. DOI: org/10.1007/s13296-017-6008-6.
66. Mohammadi, Y., Bagheripourasil, M. "Investigation of steel buildings response equipped with buckling-restrained braces against progressive collapse", *Journal of Structural and Construction Engineering (JSCE)*, Vol. 8, No. 2, (2019), 119-140, DOI: 10.22065/jsce.2019.153064.1688.
67. Guo, L., Gao, S., Fu, F., Wang, Y. "Experimental study and numerical analysis of progressive collapse resistance of composite frames." *Journal of Constructional Steel Research*, Vol. 89, (2013), 236-251.
68. Floruț, S. C., Sas, G., Popescu, C., Stoian, V. "Tests on reinforced concrete slabs with cut-out openings strengthened with fiber-reinforced polymers." *Composites Part B: Engineering*, Vol. 66, 484-493, DOI: 10.1016/j.compositesb.2014.06.008.
69. Ellobody, E., Bailey, C. G. "Modeling of unbonded post-tensioned concrete slabs under fire conditions." *Fire Safety Journal*, Vol. 44, No. 2, (2009), 159-167.
70. Nawy, E. G. (1996). Prestressed concrete. A fundamental approach (No. Second Edition).
71. Kong, F. K., Evans, R. H. "Reinforced and prestressed concrete.", (2013), DOI: 10.1017/CBO9781107282223.
72. Ma, G., Du, Q. "Structural health evaluation of the prestressed concrete using advanced acoustic emission (AE) parameters." *Construction and Building Materials*, Vol. 250, (2020), 118860, DOI: 10.1016/j.conbuildmat.2020.118860.
73. Wu, C., Oehlers, D. J., Rebstrost, M., Leach, J., Whittaker, A. S. "Blast testing of ultra-high-performance fiber and FRP-retrofitted concrete slabs." *Engineering Structures*, Vol. 31, No. 9, (2009), 2060-2069.
74. Mosallam, A. S., Mosalam, K. M. "Strengthening of two-way concrete slabs with FRP composite laminates." *Construction and building materials*, Vol. 17, No. 1, (2003), 43-54.
75. Hassan, T., Rizkalla, S. "Flexural strengthening of prestressed bridge slabs with FRP systems." *PCI Journal*, Vol. 47, No. 1.
76. Abdulrahman, B. Q., Aziz, O. Q. "Strengthening RC flat slab-column connections with FRP composites: A review and comparative study." *Journal of King Saud University-Engineering Sciences*, Vol. 33, No. 7, (2021), 471-481. DOI: 10.1016/j.jksues.2020.07.005.

## Persian Abstract

## چکیده

یکی از موضوعاتی که در زمینه خرابی پیش‌رونده‌ی ساختمان‌های فولادی، توجهی کمتری به آن شده است، بررسی اثر وجود بازشوی سقف بر پاسخ این ساختمان‌ها در برابر احتمال وقوع خرابی پیش‌رونده می‌باشد. در این مطالعه به بررسی تحلیلی اثر سطح و موقعیت بازشوی سقف بتن مسلح بر پتانسیل خرابی پیش‌رونده ساختمان‌های فولادی پرداخته شد. همچنین دو راهکار جهت بهسازی و مقاوم سازی دال‌های دو طرفه بتنی در برابر خرابی پیش‌رونده پیشنهاد شد. به منظور بهسازی از دال‌های بتنی پیش‌تنیده استفاده شد و به منظور مقاوم سازی، روش نصب ورق‌های CFRP بر روی سطح دال بتنی قدیمی بکار برده شد. مدلسازی با استفاده از روش اجزاء محدود و نرم افزار ABAQUS انجام شد. صحت روش شبیه‌سازی مورد استفاده با مدلسازی مطالعات آزمایشگاهی مختلف ارزیابی شد و تطابق مناسبی بین نتایج آزمایشگاهی و شبیه‌سازی اجزاء محدود مشاهده شد. ابعاد بازشویهای سقف به ترتیب  $4 \times 10$  و  $6 \times 12$  متر مربع و موقعیت آنها در گوشه و وسط پلان در نظر گرفته شد. نتایج حاصل از تحلیل خرابی پیش‌رونده نشان داد در ساختمان‌های فولادی با سیستم قاب خمشی، هنگامی که ستون‌های گوشه حذف می‌شوند و بازشوها در وسط پلان سازه قرار دارند، نیروهای محوری ستون‌های اطراف محل حذف، بسته به نوع سقف در نظر گرفته شده ۱۸ تا ۲۰ درصد بیشتر از مقادیر متناظر با حالت‌های وجود بازشو در گوشه پلان می‌باشند. همچنین افزایش ابعاد بازشو از  $4 \times 10$  متر مربع به  $6 \times 12$  متر مربع، بسته به موقعیت قرارگیری بازشو و نوع سقف در نظر گرفته شده، نیروی محوری ایجاد شده در اطراف محل حذف را حدوداً ۱۲ تا ۱۹ درصد افزایش داد. از بین دال‌دو طرفه بتن مسلح، دال بتن مسلح پیش‌تنیده و دال دو طرفه بتن مسلح مقاوم سازی شده با CFRP، دال‌های پیش‌تنیده بهترین عملکرد را داشتند؛ بطوریکه نیروهای محوری اطراف محل حذف متناظر با آنها بسته به موقعیت و ابعاد بازشو در حدود ۲۷ تا ۳۵ درصد کمتر از مقادیر متناظر با دال‌های دو طرفه شد. در دال‌های بتنی پیش‌تنیده تاندون‌های با مقاومت کششی بالا بجای آرماتورهای معمولی قرار می‌گیرند و در دو انتها توسط گره‌های مخصوص به تیر تثبیت می‌شوند. این کابل‌ها تحت کشش زیادی قرار می‌گیرند و پس از رها شدن از کشش، تمایل به جمع شدن و رسیدن به حالت اولیه دارند. بنابراین نیروی فشاری زیادی در قسمت زیرین تار ختنی در بتن ایجاد می‌شود. این نیروهای فشاری در مقابل نیروهای کششی که به واسطه بارهای ثقلی در بتن ایجاد می‌شود، قرار می‌گیرند و مقداری از نیروهای ناشی از بارهای ثقلی را ختنی می‌نمایند و بدین ترتیب پتانسیل سازه در برابر خرابی پیش‌رونده کاهش می‌یابد.